

Superhydrophobic Cuprous Oxide Nanostructures on Phosphor-Copper Meshes and Their Oil–Water Separation and Oil Spill Cleanup

Ling-Hao Kong,^{†,‡} Xin-Hua Chen,[§] Lai-Gui Yu,[†] Zhi-Shen Wu,[†] and Ping-Yu Zhang^{*,†}

[†]Key Laboratory of Ministry of Education for Special Functional Materials, Henan University, Kaifeng 475004, People's Republic of China

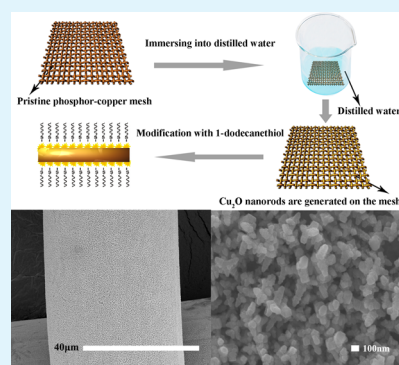
[‡]Rizhao Environmental Monitor Station, Rizhao 276800, People's Republic of China

[§]School of Chemistry and Chemical Engineering, Xuchang University, Xuchang 461000, People's Republic of China

Supporting Information

ABSTRACT: A simple aqueous solution-immersion process was established to fabricate highly dense ordered Cu₂O nanorods on commercial phosphor-copper mesh, with which the preparation was accomplished in distilled water. The present method, with the advantages of simple operation, low cost, short reaction time, and environmental friendliness, can be well adopted to fabricate desired Cu₂O nanostructures on the phosphor-copper mesh under mild conditions. After surface modification with 1-dodecanethiol, the Cu₂O nanostructure obtained on the phosphor-copper mesh exhibits excellent superhydrophobicity and superoleophilicity. Besides, a “mini boat” made from the as-prepared superhydrophobic phosphor-copper mesh can float freely on water surface and in situ collect oil from water surface. This demonstrates that the present approach, being facile, inexpensive, and environmentally friendly, could find promising application in oil–water separation and off shore oil spill cleanup.

KEYWORDS: phosphor copper mesh, cuprous oxide nanostructure, wettability, oil spill cleanup



1. INTRODUCTION

The Gulf of Mexico oil spill is one of the most serious pollution incidents of the last decades in the world: it released about 4.9 million barrels of crude oil into the ocean and brought wide and serious damage to the ocean and coast near the oilfield. To deal with such oil spills and reduce relevant environmental pollution, scientists have made great efforts to pursue materials and technologies that are applicable to efficiently separating oil and water.¹ Among various materials for such a purpose, superhydrophobic absorbent materials, with excellent selective absorption ability, fast absorption kinetics, and excellent repeatability, are of particular significance.^{2–4} To date, superhydrophobic absorbent materials can be fabricated by various approaches such as chemical vapor deposition,^{5–7} template method,^{8–11} phase inversion,¹² chemical etching,^{13,14} self-assembly,^{15,16} sol–gel process,^{17–20} electrospinning, and so forth.^{21–26} Deng and co-workers reported that superhydrophobic conjugated microporous polymers not only possess good absorbencies for oils and nonpolar organic solvents but also exhibit good absorbencies for toxic or polar organic solvent.²⁷ Xie and co-workers prepared a kind of monodisperse porous polysulfone microsphere that can absorb motor oil up to 33.6 times its self-weight.²⁸ Athanassiou and co-workers reported that a type of polyurethane foam fabricated by a solvent-free, electrostatic polytetrafluoroethylene particle dep-

osition technique exhibits water-repellent and oil-absorbing capabilities as well as magnetic responsiveness.²⁹

The above-mentioned materials can achieve high efficient oil–water separation, but the preparing methods, unfortunately, are usually time-consuming and cost-ineffective and rely on specific equipment as well as chemicals including strong acid, strong alkali, and even toxic reagents, which greatly hinders their practical applications. This is why it is imperative to pursue facile, inexpensive, and environmentally friendly methods for fabricating functional absorbent materials.

We pay special attention to superhydrophobic porous materials that can realize oil/water separation through filtrating or absorbing oil from the oil–water mixtures.^{30–35} Polytetrafluoroethylene (PTFE) coated stainless steel mesh, reported by Feng and co-workers, is an example of such superhydrophobic porous materials. As-prepared PTFE-coated stainless steel mesh integrates superhydrophobicity with superoleophilicity, and it allows the spread and permeation of diesel oil droplet as well as successful separation of the mixture of diesel oil and water.³⁵ Following Feng's work, many researchers have fabricated numerous functional materials with excellent separation performance by a variety of methods. For example, Deng et

Received: November 3, 2014

Accepted: January 15, 2015

Published: January 15, 2015

al. used a dip coating method to prepare a functionally integrated device that can continuously clean up spilled oil on the water surface.³⁶ Shi and co-workers, by combining electroless metal deposition³⁷ with monolayer self-assembly technique, fabricated multifunctional nickel foam, which could be used as a multifunctional device that integrates with the functions of oil containment booms, oil-sorption materials, oil skimmers, and water–oil separating devices.³⁸ Li and co-workers used a thermal oxidation process to fabricate a functional miniature device based on a superhydrophobic and superoleophilic mesh, and the as-obtained smart device could in situ adsorb, contain, and collect a variety of oils from water surface via capillary action and gravitational effect.³⁹ The annealing method adopted by them, however, relies on heating at elevated temperature to transform copper to cuprous hydroxide, thereby adding to more energy consumption. Recently, several researchers reported a kind of smart oil collecting device,^{40–42} which can achieve a more efficient oil spill cleanup. For instance, Wang et al. adopted a dip-coating method to fabricate a polyester-based functional sponge, which could separate large amounts of oils (up to 35 000 times its own weight) from water surface in a one-step process.⁴¹ Ge et al. described an oil collection apparatus based on the combination of porous hydrophobic and oleophilic materials with pipes and a self-priming pump and realized consecutive in situ collection of oil from water surface with high speed and efficiency.⁴² Nevertheless, it still remains a challenge to pursue a simple and green method to fabricate functional absorbent materials for oil–water separation and oil spill cleanup.

Cu₂O film has attracted extensive attention, due to its potential applications in photovoltaic devices,^{43–45} catalysis,^{46–48} photoelectrochemical cells,^{49,50} lithium ion battery,^{51,52} water splitting,⁵³ and so on. Thermal oxidation,^{44,52,54} chemical vapor deposition,⁵⁵ hydrothermal process,⁴⁸ and electrodeposition^{43,46,47,51,53,56} have been widely applied to fabricate various cuprous oxide films on different substrates. These methods, however, have disadvantages such as a complicated operating process,⁵³ high reaction temperature,^{43,46,48} high cost,⁴⁵ and low environmental acceptability.⁵⁴ Jayewardena et al. and Fernando et al., by making use of a simple solution-immersion route at 40 °C, separately obtained Cu₂O films.^{57,58} However, the as-obtained Cu₂O layer is loose and random. Thus, it is promising to fabricate highly dense ordered Cu₂O films at room temperature by a facile, inexpensive, and environmentally friendly method.

In the present research, we simply immerse phosphor-copper mesh in distilled water at room temperature to deposit high-density of ordered Cu₂O rod-like nanostructures. The whole process is completed in distilled water in the absence of any other chemical reagents. After surface modification with 1-dodecanethiol, the mesh with Cu₂O nanostructures shows excellent superhydrophobicity and superoleophilicity. The present method, with the advantages of simple operation, low cost, short reaction time, and environmental friendliness, could help to offer a facile and environmentally friendly route for fabricating functional absorbent materials with potentials for oil–water separation and off shore oil spill cleanup.

2. EXPERIMENTAL SECTION

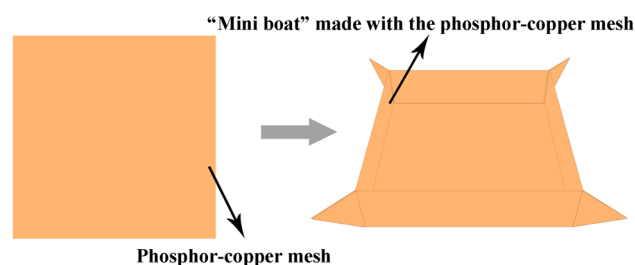
Materials. Phosphor-copper mesh was purchased from Jiuji Wire Mesh Products Co. Ltd. (Anping, China; the phosphor-copper wire has a diameter of 0.05 mm (200 mesh per inch), a copper content of 85–90% (mass fraction; the same hereafter), and a tin content of 5–

15%). Copper mesh (copper content 99.9%) was purchased from Sinopharm Chemical Reagent Co. Ltd. (Beijing, China).

Preparation of Superhydrophobic and Oleophilic Phosphor-Copper Mesh. Phosphor-copper mesh with a size of 10 mm × 20 mm was sequentially cleaned ultrasonically in acetone and 0.1 mol L⁻¹ HNO₃ aqueous solution to thoroughly remove surface impurities. The cleaned phosphor-copper mesh was immersed in distilled water at different temperatures for different reaction durations to deposit Cu₂O nanostructures. Resultant phosphor-copper mesh with Cu₂O nanostructures was rinsed with distilled water and dried with nitrogen, followed by immersion in the ethanol solution of 1-dodecanethiol (C₁₂H₂₅-SH, Sinopharm Group Chemical Reagent C. Ltd.; approximately 0.01 M) for 18 h. At the end of immersion in the ethanol solution of C₁₂H₂₅-SH, the phosphor-copper mesh was rinsed with ethanol and dried with nitrogen, followed by storing in an oven (60 °C) for 30 min to achieve superhydrophobicity and superoleophilicity.

Preparation of Superhydrophobic and Oleophilic “Mini Boat”. As shown in Scheme 1, a phosphor-copper mesh sheet (5.0

Scheme 1. Schematic Diagram Showing the Fabrication of the “Mini Boat”

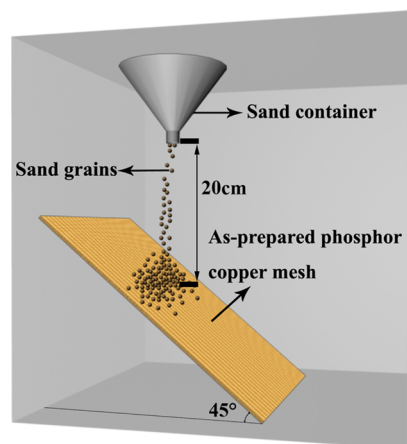


cm × 5.0 cm) is enfolded into the boat with a size of 3.4 cm × 3.4 cm × 0.8 cm, and the “mini boat” is then immersed in distilled water to grow Cu₂O nanorods. Resultant Cu₂O nanostructure is finally modified with 1-dodecanethiol to provide superhydrophobic and superoleophilic boat-like mesh, “mini boat”.

Sand Impact Tests of As-Prepared Phosphor-Copper Mesh.

To estimate the mechanical strength of as-prepared phosphor-copper mesh, we conducted sand impact tests as shown in Scheme 2. Briefly,

Scheme 2. Schematic Illustration of Sand Abrasion Experiment



sand grains were introduced to impact the surface of the as-prepared Cu₂O nanostructure from a height of 20 cm, and the contact angle (CA) of the as-prepared phosphor-copper mesh after sand impact tests was measured to estimate the physical and mechanical stability of the mesh.

The Recycled Experiments of Oil–Water Separation. The recycled experiments were carried out by the following process. As

Scheme 3. Schematic Illustration of the Formation of Superhydrophobic Phosphor-Copper Mesh

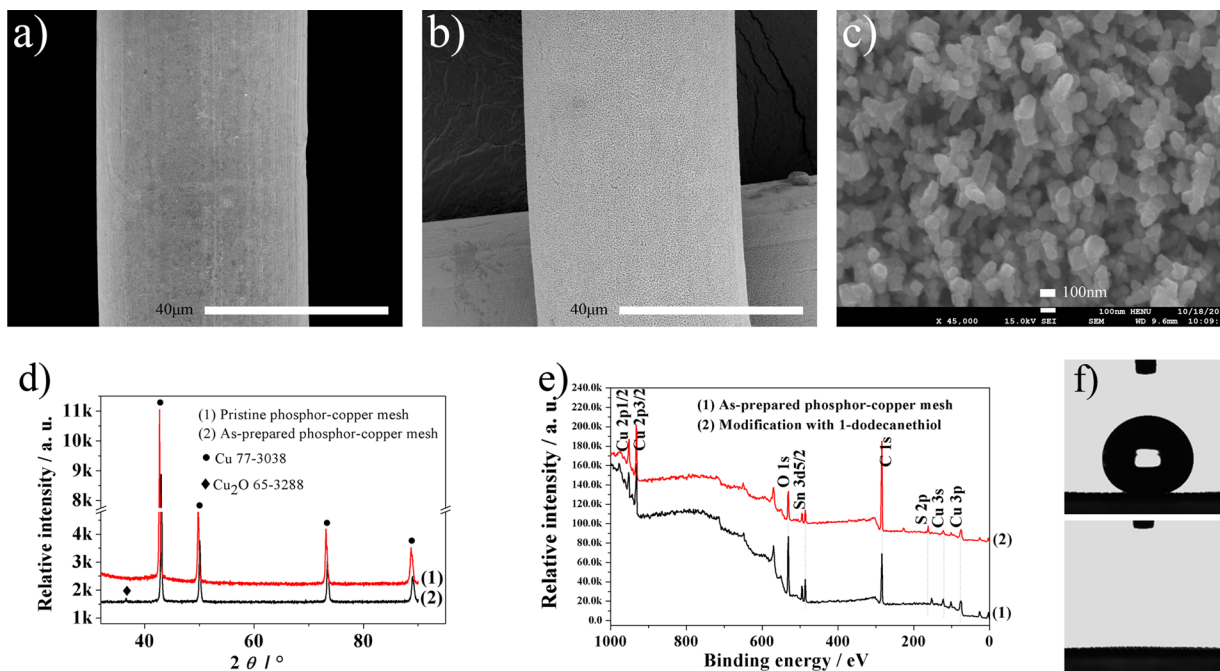
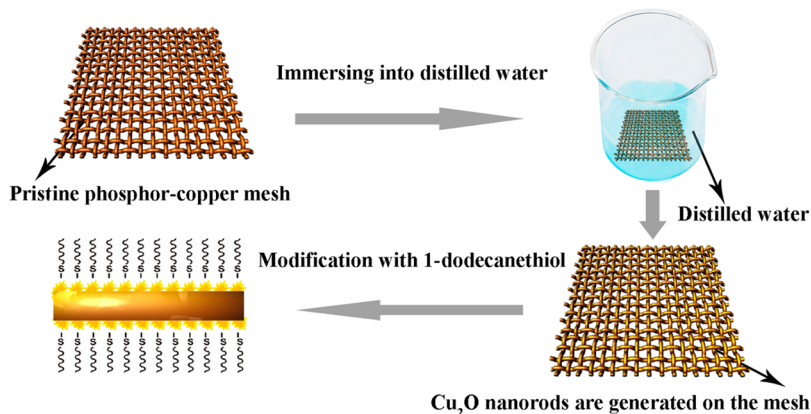


Figure 1. (a) SEM image of pristine phosphor-copper mesh; (b,c) SEM image and high-magnification SEM image of Cu_2O nanostructure (prepared at a room temperature of 25°C and a reaction time of 3 h) on phosphor-copper mesh; (d) XRD patterns of the phosphor-copper mesh before (1) and after (2) construction of Cu_2O nanostructure; (e) XPS survey spectra of Cu_2O nanostructures (room temperature 25°C , reaction time 3 h) on phosphor-copper mesh before (1) and after (2) being modified with 1-dodecanethiol; and (f) photograph of the water droplet with a contact angle of $(162.0 \pm 1.4)^\circ$ (up) and an oil droplet with a contact angle of nearly zero (down) on as-prepared superhydrophobic and superoleophilic phosphor-copper mesh.

shown in Figure 6a,b, the water–diesel oil mixture was well separated. The “mini boat” was carefully washed with ethanol three times and dried in the oven at 60°C . The as-dried “mini boat” was finally placed in the beaker to repeat the separating process.

Characterization of As-Prepared Phosphor-Copper Mesh.

The morphology of as-prepared Cu_2O nanostructures modified with 1-dodecanethiol was observed using a scanning electron microscope (SEM, JSM-7001LV, JEOL Ltd., Japan). The composition and chemical states of the Cu_2O nanostructures before and after modification with dodecanethiol were analyzed with an Axis Ultra X-ray photoelectron spectroscope (XPS, VG Scientific ESCALAB 250, UK) equipped with a standard monochromatic Al $K\alpha$ source ($h\nu = 1486.6\text{ eV}$). The binding energy data were calibrated with respect to the C 1s signal of ambient hydrocarbons (C–H and C–C) at 284.8 eV . X-ray diffraction (XRD) patterns were obtained with a multipurpose X-ray diffractometer (D8 Advance, Bruker AXS Inc., Germany) equipped with a copper target tube and an incident beam monochromator ($\lambda = 1.5406\text{ \AA}$). The Fourier transform infrared (FT-

IR) spectra of dodecanethiol-modified Cu_2O nanostructure and dodecanethiol (the modifier) were recorded with an infrared (IR) spectrometer (AVATAR360, Nicolet, U.S.). Water contact angles at room temperature ($4.5\text{ }\mu\text{L}$ of distilled water droplet was used for the measurements) were measured with an optical contact angle meter (Dropmaster 300, Kyowa Interface Science, Japan), and at least five repeat measurements were conducted for each tested sample. A high-speed digital camera attached to the contact angle meter (JC2000D2, Shanghai Zhongchen Digital Technology Equipment Co., Ltd., Shanghai, China) was performed to record the images of the water droplet ($8\text{ }\mu\text{L}$) rolling off the surface of as-prepared Cu_2O nanostructures after modification with dodecanethiol.

3. RESULTS AND DISCUSSION

Scheme 3 presents the schematic illustration of the formation of Cu_2O nanostructure on the phosphor-copper mesh via immersion and deposition in distilled water, where the

formation of Cu_2O nanorods is completed within 3 h. After ultrasonically cleaned phosphor-copper mesh is immersed in distilled water at room temperature (about 25 °C), the mesh surface gradually changes from copper color to light yellow along with extending reaction time, which indicates that some new substances have been generated on the phosphor-copper mesh. This approach has several advantages. The whole process is completed in distilled water in the absence of chemicals such as strong acid, strong alkaline, and other environmentally unfriendly reagents, which means that the route is environmentally acceptable. Besides, the route is inexpensive and facile and does not involve special technique or special equipment, which provides feasibility to realize industrial mass production of superhydrophobic nanostructures on phosphor-copper mesh surface.

Typical scanning electron microscopic (SEM) images of the phosphor-copper meshes before and after immersing in distilled water are shown in Figure 1a,b. The pristine phosphor-copper mesh has a quite smooth surface (Figure 1a). After the phosphor-copper mesh is immersed in distilled water at 25 °C for 3 h, high density of regular and ordered nanostructure is formed on the surface (Figure 1b). The corresponding high magnification SEM image reveals that the nanostructure consists of nanorods with a diameter of about 90 nm (Figure 1c), and most of the nanorods grow into nanoclusters at an inter-angle of 90°. In such a mode of growth, the nanostructure and micrometer-sized phosphor-copper wires form a hierarchical morphology with dual-scale roughness, which helps to endow the mesh with improved wettability. Figure 1d presents the XRD patterns of the mesh before and after immersion in distilled water (25 °C, 3 h). Both original phosphor-copper mesh and the mesh with Cu_2O nanostructure show strong XRD peaks of cubic-phase Cu (marked with black dots; JCPDS card no. 77-3038), and the latter exhibits a small new diffraction peak (see the XRD peak marked with a black diamond in pattern 2 of Figure 1d) that can be well indexed to Cu_2O (JCPDS card no. 65-3288). In other words, the rod-like nanostructure formed on the surface of the mesh consists of Cu_2O nanocrystal.

Figure 1e shows the typical XPS survey spectra of Cu_2O nanostructure (25 °C, 3 h) before and after chemical treatment with 1-dodecanethiol. Both samples exhibit a Cu 3p peak at 75.1 eV, Cu 3s peak at 122.4 eV, Cu 2p doublet (Cu 2p^{3/2} at 932.4 eV and Cu 2p^{1/2} at 952.4 eV), Sn 3d^{5/2} peak at 486.1 eV, O 1s peak at 531.1 eV, and C 1s peak at 284.8 eV. The Sn 3d^{5/2} peak is attributed to the tin phase of phosphor-copper. In Supporting Information Figure S1a, the Sn 3d double peaks can be fitted into two doublets located at 486.0 eV (Sn 3d^{5/2}) and 494.5 eV (Sn 3d^{3/2}) as well as 485.2 eV (Sn 3d^{5/2}) and 493.6 eV (Sn 3d^{3/2}), and they could be attributed to surface oxidation of tin (SnO_2) and unoxidized tin below the oxide layer.^{59,60} This indicates that tin on the surface of phosphor-copper mesh is oxidized into SnO_2 upon immersion in distilled water, generating Cu_2O nanorods. Supporting Information Figure S2 shows the high-resolution XPS spectra of O 1s region of as-prepared Cu_2O nanostructures and the as-prepared Cu_2O nanostructures modified with 1-dodecanethiol. The XPS O 1s peaks can be fitted into two peaks located at ca. 530.3 and 532.0 eV (531.7 eV), which are attributed to the lattice oxygen of Cu_2O and surface-adsorbed oxygen species.⁶¹ This indicates that as-prepared phosphor-copper mesh has a large amount of oxygen species adsorbed on the surface, which could be because the nanorods on the surface possess many corners and steps that

offer a large surface area and abundant adsorption sites. The peak located at ca. 530.3 eV corresponds to Cu_2O nanostructure, it is found before and after chemical treatment with 1-dodecanethiol, and its intensity decreases significantly after the modification, due to chemical reaction. The C 1s peak at 284.8 eV corresponds to contaminant carbon and/or carbon of dodecanethiol, and its intensity increases significantly after the Cu_2O nanostructure is modified with dodecanethiol. This primarily proves that chemical adsorption and/or chemical bonding take place upon the modification of the Cu_2O nanostructure by dodecanethiol, which is further confirmed by corresponding FT-IR data. As shown in Figure 2, the

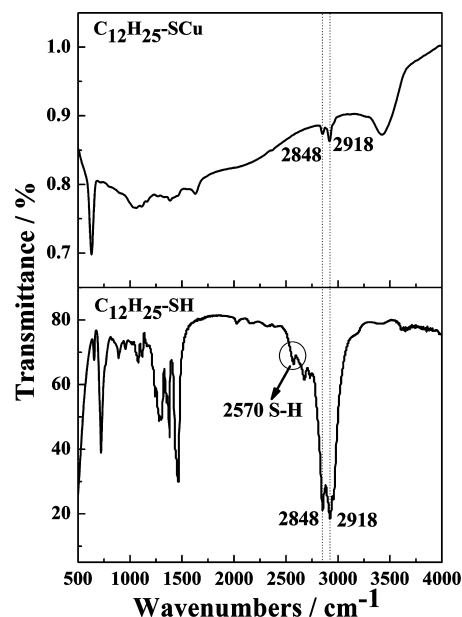
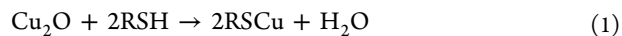


Figure 2. FT-IR spectra of Cu_2O nanostructure modified with dodecanethiol (upper part) and modifier dodecanethiol (lower part).

absorption band at 2850–2920 cm^{-1} is attributed to the C–H stretch vibration of $-\text{CH}_3$ and $-\text{CH}_2-$, and the one at 2570 cm^{-1} is assigned to the stretching vibration of S–H. Interestingly, Cu_2O nanostructure modified with dodecanethiol does not show the S–H stretching vibration at 2570 cm^{-1} , which implies that S–H is destroyed and S atom is anchored on the surface of Cu_2O nanostructure via strong interaction.⁶²

To further reveal the chemical state of S in the as-prepared Cu_2O nanostructure modified by dodecanethiol, we collected high-resolution XPS data of S element. The S 2p XPS spectrum of the phosphor-copper mesh containing Cu_2O nanostructure modified by dodecanethiol can be fitted into three major peaks (see Supporting Information Figure S1b). The S 2p peak at 162.3 eV is assigned to the RS–Cu group that is formed upon the chemical reaction between RSH and Cu(I) by the following eq 1:⁶³



Meanwhile, as shown in eq 2, disulfide RS–SR is also generated during the reaction of RSH with Cu_2O .⁶⁴ The S 2p peak centered at 163.1 eV is originated from disulfide that can be physically adsorbed on the surface of the mesh,⁶⁵ and the S 2p peak at 163.6 eV is attributed to the unbound thiols.⁶⁶ These XPS data give further evidence to the conclusion that the rod-

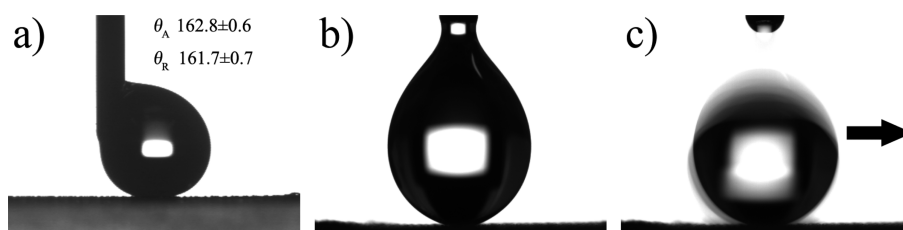


Figure 3. (a) Advancing/receding contact angle (denoted as θ_A and θ_R) of phosphor-copper mesh with Cu_2O nanostructure obtained at 25 °C and 3 h. Diagrams showing the contact process of a water droplet (8 μL) on the surface of phosphor-copper mesh: (b) right upon contact, (c) after 0.040 s of contact (the sliding angle less than 1°). The arrow represents the moving direction of the water droplet.

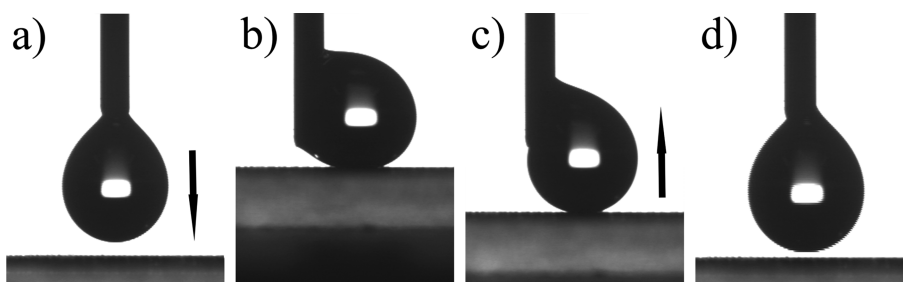


Figure 4. Approach, contact, deformation, and departure processes of a 4 μL water droplet suspended on a syringe with respect to superhydrophobic Cu_2O nanostructure obtained at 25 °C and 3 h. The arrows represent the moving direction of the water droplet in relation to the substrate.

like nanostructure formed on the surface of phosphor-copper mesh is composed of Cu_2O nanocrystal.

Moreover, as shown in Figure 1f, the water droplet on the dodecanethiol-modified rod-like Cu_2O nanostructure looks like a sphere, and its water contact angle is as much as $(162.0 \pm 1.4)^\circ$, corresponding to excellent superhydrophobicity. Meanwhile, diesel oil, a liquid with low surface tension, spreads quickly on the dodecanethiol-modified rod-like Cu_2O nanostructure mesh and permeates it thoroughly, corresponding to high oleophilicity. This indicates that as-prepared Cu_2O nanostructure modified with dodecanethiol exhibits superhydrophobicity and superoleophilicity.

The formation mechanism of rod-like Cu_2O nanostructures on the surface of phosphor-copper mesh in distilled water was also investigated. First, we put the pretreated phosphor-copper mesh (the pretreatment involves two stages: the removal of organic substances on the surface by acetone and the removal of the oxides thereon by HNO_3 aqueous solution) into double distilled water, and we found that the trace substances in the double distilled water have no significant effects on the formation reaction of rod-like Cu_2O nanostructures therein (see Supporting Information Figure S3a). Second, we put the copper mesh pretreated with the same process into distilled water, but we found that no Cu_2O crystal is formed on the surface of the copper mesh (see Supporting Information Figure S3b). Third, we cleaned the phosphor-copper mesh in acetone to remove organic substances but did not clean it in HNO_3 aqueous solution to remove the oxides, and in this case we failed to obtain rod-like Cu_2O nanostructures (see Supporting Information Figure S3c). This indicates that some ingredients in the phosphor-copper mesh may catalyze the formation of Cu_2O crystal, and the oxides on the surface of the phosphor-copper mesh prevent the chemical reaction from igniting. We conducted further experiments to clarify whether the oxygen originated from water or the oxygen dissolved in water is responsible for the oxidation process of the phosphor-copper mesh therein, and we found that no Cu_2O nanorods are formed in the dissolved oxygen-free water. This demonstrates that

dissolved oxygen in water plays a key role in the oxidation process of the pretreated phosphor-copper mesh, and it could be feasible to well manipulate the formation of Cu_2O crystal by properly controlling the amount of dissolved oxygen. Moreover, it is critical to identify the role of the tin phase in the oxidation process. In the pretreatments, the oxide layer of the phosphor-copper mesh is removed by cleaning with HNO_3 aqueous solution, while the tin phase is partly dissolved to generate many pits. Upon immersion of the cleaned phosphor-copper mesh in distilled water, the tin phase is oxidized first, due to its higher activity than copper, and the Cu_2O nanostructures may form through the mechanism similar to localized corrosion in copper tubes.⁶⁷ The pits on the phosphor-copper mesh surface may function as microanodes for copper dissolution and the adjacent copper phase as microcathodes for oxygen reduction, thereby allowing preferential oxidation at the defects (i.e., the pits) through the anodic reaction described in eq 3 and cathodic reaction described in eq 4:



The OH^- ions formed at the cathode can migrate and diffuse toward the anode to form Cu_2O through eqs 5 and 6:



Cu_2O tends to preferentially nucleate at the defects on the phosphor-copper mesh surface and gradually grow. Nevertheless, it still remain unknown why the oxidation process is so fast and how the two phases of the metals influence each other in the oxidation process. Further work is to be conducted to clarify these issues.

A very high static water contact angle in association with a very low sliding angle is referred to as the “lotus effect”.^{68,69} The so-called “lotus effect” means that small droplets with very

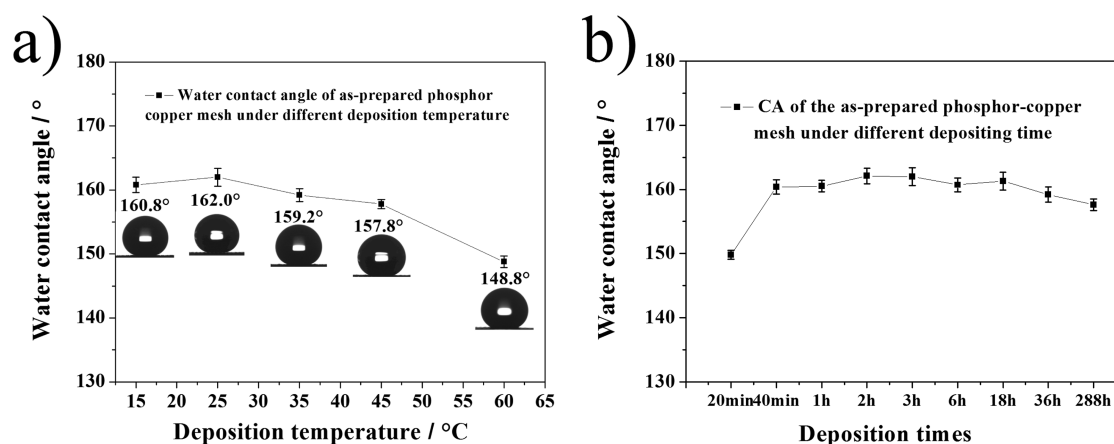


Figure 5. (a) Dynamic water contact angle measurements on superhydrophobic phosphor-copper mesh modified with 1-dodecanethiol under deposition temperatures of 15, 25, 35, 45, and 60 °C; insets are corresponding photographs of the water contact angle. (b) Dynamic water contact angle measurements on superhydrophobic phosphor-copper mesh modified with 1-dodecanethiol under deposition times of 20 min, 40 min, 1 h, 2 h, 3 h, 6 h, 18 h, 36 h, and 288 h.

low adhesion can easily roll off solid surface and carry away dirt, thereby realizing self-cleaning. Aside from the static contact angle measurements of the Cu_2O nanostructures prepared in distilled water at 25 °C, the wetting behavior of the as-prepared Cu_2O nanostructures was also analyzed by contact angle hysteresis. As shown in Figure 3a, as-prepared Cu_2O nanostructures exhibit very high advancing/receding contact angles of $(162.8 \pm 0.6)^\circ$ and $(161.7 \pm 0.7)^\circ$ as well as a low contact angle hysteresis of $(1.2 \pm 0.2)^\circ$, showing good superhydrophobicity. Meanwhile, the water droplet rolls off the superhydrophobic mesh surface within a very short time (about 0.040 s) while the mesh is not tilted at all (see Figure 3b,c and Supporting Information videos S1 and S2). Naturally, such an “easy rolling” characteristic of the water droplet on as-prepared superhydrophobic mesh surface adds difficulty to the contact angle measurements. To deal with this issue, we carefully stick macroscopically rough phosphor-copper mesh onto a glass substrate with a double-sided adhesive. Even so, the water droplet still can easily roll off during water angle measurements, which demonstrates that as-prepared superhydrophobic nanostructure on the phosphor-copper mesh exhibits a very low sliding angle. Figure 4 shows the contact, deformation, and departure processes of a 4 μL water droplet suspended on a syringe with respect to the as-prepared superhydrophobic surface. It can be seen that the water droplet can almost completely detach from the substrate even upon severe deformation. Such an excellent superhydrophobicity should be closely related to the surface morphology and the special chemical composition of the as-prepared nanostructure. The mesh is composed of phosphor-copper wires with a diameter of about 40 μm , and the phosphor-copper wires are interweaved with each other to form a micrometer-sized rough surface. Immersion of the rough pristine phosphor-copper mesh in distilled water produces Cu_2O nanorods, thereby providing a dual-scale roughness surface. After introduction of 1-dodecanethiol with low surface free energy, such a dual-scale roughness structure can bring a sufficient proportion of trapped air to the surface and largely increase the repellent force to water, resulting in stable superhydrophobicity in association with a very low sliding angle and nearly zero adhesion to water droplet. As a result, the water droplet is able to instantly roll off the superhydrophobic mesh surface and eliminate dirt thereon,

thereby resulting in self-cleaning of the mesh surface (see Supporting Information video S3).

It is cheap and facile to fabricate nanostructures on metal substrate by solution-immersing technique, but this method always needs to accurately control the deposition temperature and solution concentration, which play important roles in crystal growth.^{70–72} We also conducted studies in this respect. As shown in Figure 5a, superhydrophobic Cu_2O nanostructures prepared under deposition temperatures of 15, 25, 35, 45, and 60 °C exhibit water contact angles of $(160.8 \pm 1.2)^\circ$, $(162.0 \pm 1.4)^\circ$, $(159.2 \pm 1.0)^\circ$, $(157.8 \pm 0.7)^\circ$, and $(148.8 \pm 0.9)^\circ$, respectively (the averages of the five repeat measurements of contact angles are provided, and the numerals following “ \pm ” refer to standard measurement deviations). Besides, varying deposition temperature from 15 to 45 °C leads to few changes in the superhydrophobicity of as-prepared Cu_2O nanostructure modified by 1-dodecanethiol. In other words, the present approach could be promising for large-scale commercial application of superhydrophobic Cu_2O nanostructure on phosphor-copper mesh, because it is applicable in a wide range of reaction temperatures. Yet, as the immersing temperature increased to 60 °C, the water contact angles of the mesh would rapidly drop to $(148.8 \pm 0.9)^\circ$. This indicates that too high of an immersing temperature will greatly affect the hydrophobicity performance of the surface. The high-magnification SEM images of superhydrophobic Cu_2O nanostructures on phosphor-copper mesh obtained under different deposition temperatures provide further evidence to the influence of reaction temperature on the growth and size of Cu_2O nanostructures (see Supporting Information Figure S4). As the reaction temperature increases from 15 to 25 °C, the diameter of the Cu_2O nanorods increases (see images a and b of Supporting Information Figure S4). Besides, block-like Cu_2O nanostructure starts to appear on the surface of the mesh after it is immersed in distilled water at 35 °C (see image c of Supporting Information Figure S4). The block-like Cu_2O nanostructure tends to agglomerate into nanoclusters with increased sizes when the reaction temperature further rises to 45 °C. At a higher immersing temperature of 60 °C, the diameter of the nanoclusters increases to 200–800 nm; meanwhile, the rod-like nanostructures disappear on the surface, thereby leading to a sharp decrease of the water contact angle. Deposition time is another factor that has an

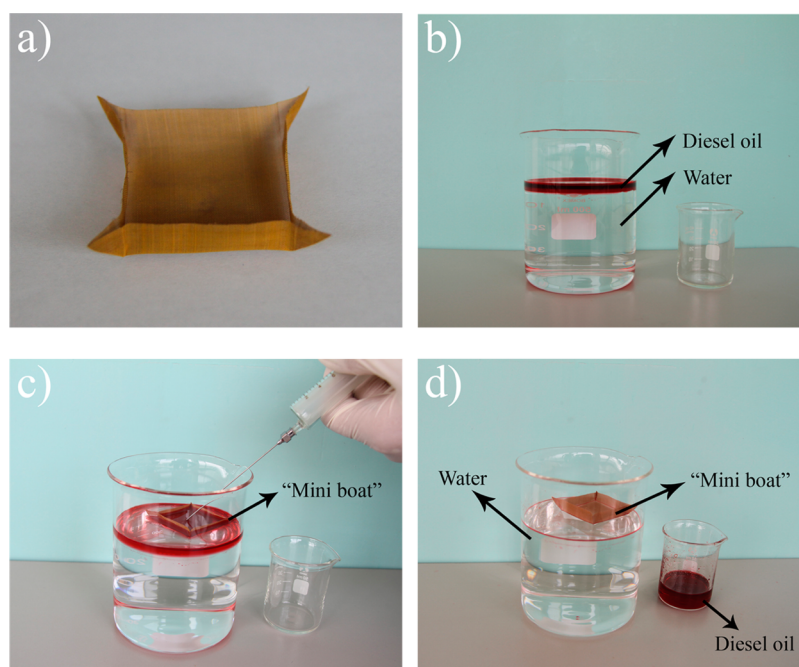


Figure 6. (a) As-prepared “mini boat”; (b–d) processes of separating diesel oil from water by using the as-prepared “mini boat”.

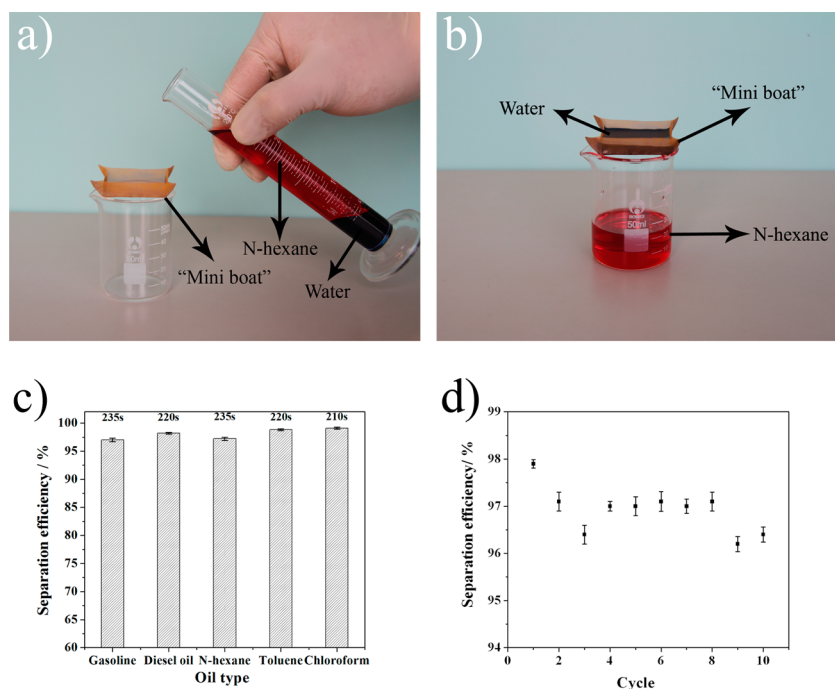


Figure 7. (a,b) Simple experiment designed to separate the mixture of *n*-hexane and water, (c) separating efficiency of different types of oil or organic solvents (the separation time of the “mini boat” for various oil–water mixtures is given at the top of the image), and (d) recycled experiments for separating oil from water by using the “mini boat”.

important influence on the crystal growth and surface morphology. Figure 5b shows the dynamic water contact angle measurements on superhydrophobic Cu_2O nanostructure modified with 1-dodecanethiol prepared under different deposition times (from 20 min to 288 h). It is seen that the water contact angle of the superhydrophobic nanostructures rises from $(149.8 \pm 0.7)^\circ$ to $(160.4 \pm 1.1)^\circ$ when the deposition time extends from 20 to 40 min, but further extending the deposition time from 40 min to 288 h leads to few changes in the water contact angle. This means that the

growth of the superhydrophobic Cu_2O nanostructure on the phosphor-copper mesh can be completed within a quite short deposition time (about 40 min), which is also confirmed by relevant Supporting Information (see Figure S5). Cu_2O nanorods with nonuniform sizes are generated on the surface of the phosphor-copper mesh after it is immersed in distilled water for 20 min (see Supporting Information Figure S5a), and the Cu_2O nanorods grow into a uniform and dense nanostructure after 40 min of immersion in the distilled water (see Supporting Information Figure S5b). As the

deposition time continues to increase, the diameter and length of the Cu_2O nanorods rise (some of them even have a length of $1.5\ \mu\text{m}$), and most of them have grown many split ends like branches. As can be seen from Supporting Information Figure S5e–h, the so-called “dendrite structure” becomes more dense when the reaction time extends from 3 to 36 h; meanwhile, the surface morphology of the nanostructure remains nearly unchanged. When the immersing time is extended to 288 h, agglomerated particles emerge on the surface of the mesh, but the contact angle of the surface changes slightly.

Nowadays, the pollution of seawater by oil is one of the most serious environmental problems worldwide. Particularly, an off shore oil spill adds difficulty to the treatment and collection of the contaminated oil. Although superhydrophobic and superoleophilic meshes can be used to efficiently separate oil contaminants from water, rare examples are currently available about their direct applications in dealing with large-scale off shore oil spills, which is partly due to the difficulty in collecting and filtering a huge amount of seawater contaminated by oil. Viewing this situation, we expect that the present approach could be adopted to prepare a boat-like superhydrophobic and superoleophilic mesh that can float on seawater, thereby providing a solution to clean up off shore oil contamination. For this purpose, a “mini boat” was prepared from the phosphor-copper mesh (see Scheme 1 and Figure 6a). To evaluate the cleanup capability of the “mini boat”, we conducted a simulation test as illustrated in Figure 6b, where the diesel oil labeled with oil red dye (a tracer) was dropped into the water to simulate oil pollution. It can be seen that the “mini boat” can float freely on the water and the diesel oil can easily permeate into it while water is excluded. After the diesel oil trapped in the “mini boat” is taken away continuously with a glass syringe (see Figure 6c,d), remnant diesel oil can continuously pass through the mesh into the “mini boat”. In this way, most of the oil pollutant is well collected (Supporting Information video S4 illustrates the whole cleanup process). Hopefully, as-prepared “mini boat” could find promising applications in dealing with off shore oil spill, and it could be of particular significance because there is no need to collect the oil-contaminated seawater while the “mini boat” can float on seawater to allow direct collection of the oil contaminant via permeation. In other words, the oil contaminant can be filtered at the oil spill site, which should help to decrease the production cost and increase the efficiency of cleanup.

In addition to its oil collection capability, the “mini boat” can also be used as an oil–water separator. For this purpose, we designed a simple experiment to evaluate the oil/water separation capability of the “mini boat”. As shown in Figure 7a, the “mini boat” is put on a beaker, and then the mixture of water and *n*-hexane (dyed with methyl blue and oil red, respectively, for easy observation) is poured into the beaker through the “mini boat”. Obviously, the *n*-hexane quickly penetrates through the “mini boat” and flows into the beaker while water remains in the “mini boat” (see Figure 7b). This indicates that the “mini boat” can easily separate oil–water mixtures. We further investigated the separation efficiency of the “mini boat” by collecting and weighing the oil passing through the “mini boat”. The separation efficiency is defined as the mass ratio of the oil collected from the beaker to that in the original oil–water mixture. As shown in Figure 7c, different types of oils such as gasoline, diesel oil, *n*-hexane, toluene, and chloroform (the surface tension of various tested oils is listed in Supporting Information Table S1) can be separated by the

“mini boat” at an efficiency of more than 96%, and various oil–water mixtures can be well separated in 4 min.

In terms of the field application of as-prepared Cu_2O nanostructure with superhydrophobicity and superoleophilicity, it is imperative to investigate its physical and chemical stability as well as recyclability and durability. Thus, we conducted 24 h of immersion test in seawater to evaluate its corrosion resistance. It was found that, after immersion in seawater for 24 h, the Cu_2O nanostructure on the phosphor-copper mesh retains nearly unchanged water contact angle, which implies that the nanostructure exhibits good chemical stability in seawater. We also conducted sand impact tests to investigate the mechanical strength of the as-prepared Cu_2O nanostructure (in the whole process of impact test, about 35 g of sand grains was introduced to impact the surface). It was found that as-prepared Cu_2O nanostructure retains superhydrophobicity after 3 min of sand impact, although extended impinge by the sand grains leads to a gradual decrease in the water contact angle. This means that the as-prepared Cu_2O nanostructure exhibits fair ability to resist sand impact while its superhydrophobicity is retained. More importantly, the as-prepared “mini boat” retains a high separation efficiency even after it is recycled (for the separation of diesel oil and water) for more than 10 times (Figure 7d), which indicates that the superhydrophobic and superoleophilic Cu_2O nanostructure modified by 1-dodecanethiol on phosphor-copper mesh exhibits good recycling performance for oil–water separation and oil spill cleanup as well.

4. CONCLUSIONS

We have established a facile, inexpensive, and environmentally friendly approach for fabricating highly dense ordered Cu_2O nanorods on phosphor-copper mesh. The present approach is advantageous over previous ones, because it adopts distilled water as the reaction medium and works well in a wide temperature range and at a shortened reaction time. As-prepared Cu_2O nanorods modified by dodecanethiol exhibit excellent superhydrophobicity and superoleophilicity as well as good self-cleaning ability and oil–water separation capability, showing great potential for concentration and collection of oil contamination and other organic chemicals with low surface tension from water surface as well as cleanup of off shore oil spill.

■ ASSOCIATED CONTENT

Supporting Information

High-resolution XPS spectra of Sn 3d, S 2p, and O 1s regions, SEM images of Cu_2O nanostructures obtained under different deposition temperatures, and SEM images of Cu_2O nanostructures obtained under different deposition times. Video S1 and video S2 demonstrate “easy rolling” characteristics of the water droplet on as-prepared superhydrophobic mesh. Video S3 shows quickly rolling off of water droplets on as-prepared Cu_2O nanostructure; video S4 demonstrates the whole process to clean up “oil spill” with the “mini boat”. The material is available free of charge via the Internet at <http://pubs.acs.org>.

■ AUTHOR INFORMATION

Corresponding Author

*Phone: (+86)378-2968765. E-mail: pingyu@henu.edu.cn.

Notes

The authors declare no competing financial interest.

ACKNOWLEDGMENTS

We acknowledge the financial support provided by the Ministry of Science and Technology of China (project of "973" Plan, grant no. 2013CB632303), National Natural Science Foundation of China (grant nos. 21171143 and 51275154), and Ministry of Education of China (Program for Changjiang Scholars and Innovative Research Team in Universities of China, grant no. PCS IRT1126).

REFERENCES

- (1) Yip, T. L.; Talley, W. K.; Jin, D. The Effectiveness of Double Hulls in Reducing Vessel-Accident Oil Spillage. *Mar. Pollut. Bull.* **2011**, *62*, 2427–2732.
- (2) Pavia-Sanders, A.; Zhang, S. Y.; Flores, J. A.; Sanders, J. E.; Raymond, J. E.; Wooley, K. L. Robust Magnetic/Polymer Hybrid Nanoparticles Designed for Crude Oil Entrapment and Recovery in Aqueous Environments. *ACS Nano* **2013**, *9*, 7552–7561.
- (3) Ruan, C. P.; Ai, K. L.; Li, X. B.; Lu, L. H. A Superhydrophobic Sponge with Excellent Absorbency and Flame Retardancy. *Angew. Chem.* **2014**, *126*, 5662–5666.
- (4) Niu, Z. Q.; Liu, L. L.; Zhang, L.; Chen, X. D. Porous Graphene Materials for Water Remediation. *Small* **2014**, *10*, 3434–3441.
- (5) Zhang, J. P.; Seeger, S. Polyester Materials with Superwetting Silicone Nanofilaments for Oil/Water Separation and Selective Oil Absorption. *Adv. Funct. Mater.* **2011**, *21*, 4699–4704.
- (6) Crick, C. R.; Gibbins, J. A.; Parkin, I. P. Superhydrophobic Polymer-Coated Copper-Mesh; Membranes for Highly Efficient Oil–Water Separation. *J. Mater. Chem. A* **2013**, *1*, 5943–5948.
- (7) Cortese, B.; Caschera, D.; Federici, F.; Ingo, G. M.; Gigli, G. Superhydrophobic Fabrics for Oil–Water Separation through a Diamond like Carbon (DLC) Coating. *J. Mater. Chem. A* **2014**, *2*, 6781–6789.
- (8) Chen, X. W.; Hong, L.; Xu, Y. F.; Ong, Z. W. Ceramic Pore Channels with Inducted Carbon Nanotubes for Removing Oil from Water. *ACS Appl. Mater. Interfaces* **2012**, *4*, 1909–1918.
- (9) Choi, S.-J.; Kwon, T.-H.; Im, H.; Moon, D.-I.; Baek, D. J.; Seol, M.-L.; Duarte, J. P.; Choi, Y.-K. A Polydimethylsiloxane (PDMS) Sponge for the Selective Absorption of Oil from Water. *ACS Appl. Mater. Interfaces* **2011**, *3*, 4552–4556.
- (10) Chu, Y.; Pan, Q. M. Three-Dimensionally Macroporous Fe/C Nanocomposites as Highly Selective Oil-Absorption Materials. *ACS Appl. Mater. Interfaces* **2012**, *4*, 2420–2425.
- (11) Zhang, W. B.; Shi, Z.; Zhang, F.; Liu, X.; Jin, J.; Jiang, L. Superhydrophobic and Superoleophilic PVDF Membranes for Effective Separation of Water-in-Oil Emulsions with High Flux. *Adv. Mater.* **2013**, *25*, 2071–2076.
- (12) Zhang, X. Y.; Li, Z.; Liu, K. S.; Jiang, L. Bioinspired Multifunctional Foam with Self-Cleaning and Oil/Water Separation. *Adv. Funct. Mater.* **2013**, *23*, 2881–2886.
- (13) Zhang, T.; Wang, J. M.; Chen, L.; Zhai, J.; Song, Y. L.; Jiang, L. High-Temperature Wetting Transition on Micro- and Nanostructured Surfaces. *Angew. Chem.* **2011**, *123*, 5423–5426.
- (14) Peng, S.; Yang, X. J.; Tian, D.; Deng, W. I. Chemically Stable and Mechanically Durable Superamphiphobic Aluminum Surface with a Micro/Nanoscale Binary Structure. *ACS Appl. Mater. Interfaces* **2014**, *6*, 15188–15197.
- (15) Wang, Y. Q.; Shi, Y.; Pan, L. J.; Yang, M.; Peng, L. L.; Zong, S.; Shi, Y.; Yu, G. H. Multifunctional Superhydrophobic Surfaces Templated from Innately Microstructured Hydrogel Matrix. *Nano Lett.* **2014**, *14*, 4803–4809.
- (16) Guix, M.; Orozco, J.; García, M.; Gao, W.; Sattayasamitsathit, S.; Merkoçi, A.; Escarpa, A.; Wang, J. Superhydrophobic Alkanethiol-Coated Microsubmarines for Effective Removal of Oil. *ACS Nano* **2012**, *6*, 4445–4451.
- (17) Leventis, N.; Chidambareswarapattar, C.; Bang, A.; Sotiriou-Leventis, C. Cocoon-in-Web-like Superhydrophobic Aerogels from Hydrophilic Polyurea and Use in Environmental Remediation. *ACS Appl. Mater. Interfaces* **2014**, *6*, 6872–6882.
- (18) Hayase, G.; Kanamori, K.; Fukuchi, M.; Kaji, H.; Nakanishi, K. Facile Synthesis of Marshmallow-like Macroporous Gels Usable under Harsh Conditions for the Separation of Oil and Water. *Angew. Chem., Int. Ed.* **2013**, *52*, 1986–1989.
- (19) Li, R.; Chen, C. B.; Li, J.; Xu, L. M.; Xiao, G. Y.; Yan, D. Y. A Facile Approach to Superhydrophobic and Superoleophilic Graphene/Polymer Aerogels. *J. Mater. Chem. A* **2014**, *2*, 3057–3064.
- (20) Zhang, G. Y.; Li, M.; Zhang, B. D.; Huang, Y.; Su, Z. H. A Switchable Mesh for on-demand Oil–Water Separation. *J. Mater. Chem. A* **2014**, *2*, 15284–15287.
- (21) Wu, J.; Wang, N.; Wang, L.; Dong, H.; Zhao, Y.; Jiang, L. Electrospun Porous Structure Fibrous Film with High Oil Adsorption Capacity. *ACS Appl. Mater. Interfaces* **2012**, *4*, 3207–3212.
- (22) Lee, M. W.; An, S.; Latthe, S. S.; Lee, C.; Hong, S.; Yoon, S. S. Electrospun Polystyrene Nanofiber Membrane with Superhydrophobicity and Superoleophilicity for Selective Separation of Water and Low Viscous Oil. *ACS Appl. Mater. Interfaces* **2013**, *5*, 10597–10604.
- (23) Huang, M. L.; Si, Y.; Tang, X. M.; Zhu, Z. G.; Ding, B.; Liu, L. F.; Zheng, G.; Luo, W. J.; Yu, J. Y. Gravity Driven Separation of Emulsified Oil–Water Mixtures Utilizing in situ Polymerized Superhydrophobic and Superoleophilic Nanofibrous Membranes. *J. Mater. Chem. A* **2013**, *1*, 14071–14074.
- (24) Tai, M. H.; Gao, P.; Tan, B. Y. L.; Sun, D. D.; Leckie, J. O. Highly Efficient and Flexible Electrospun Carbon–Silica Nanofibrous Membrane for Ultrafast Gravity-Driven Oil–Water Separation. *ACS Appl. Mater. Interfaces* **2014**, *6*, 9393–9401.
- (25) Li, X.; Wang, M.; Wang, C.; Cheng, C.; Wang, X. F. Facile Immobilization of Ag Nanocluster on Nanofibrous Membrane for Oil/Water Separation. *ACS Appl. Mater. Interfaces* **2014**, *6*, 15272–15282.
- (26) Raza, A.; Ding, B.; Zainab, G.; El-Newehy, M.; Al-Deyab, S. S.; Yu, J. Y. In situ Cross-linked Superwetting Nanofibrous Membranes for Ultrafast Oil–Water Separation. *J. Mater. Chem. A* **2014**, *2*, 10137–10145.
- (27) Li, A.; Sun, H.-X.; Tan, D.-Z.; Fan, W.-J.; Wen, S.-H.; Qing, X.-J.; Li, G.-X.; Li, S.-Y.; Deng, W.-Q. Superhydrophobic Conjugated Microporous Polymers for Separation and Adsorption. *Energy Environ. Sci.* **2011**, *4*, 2062–2065.
- (28) Yu, Q. B.; Tao, Y. L.; Huang, Y. P.; Lin, Z. Q.; Zhuang, Y. L.; Ge, L. L.; Shen, Y. H.; Hong, M.; Xie, A. J. Preparation of Porous Polysulfone Microspheres and Their Application in Removal of Oil from Water. *Ind. Eng. Chem. Res.* **2012**, *51*, 8117–8122.
- (29) Calcagnile, P.; Fragouli, D.; Bayer, I. S.; Anyfantis, G. C.; Martiradonna, L.; Cozzoli, P. D.; Cingolani, R.; Athanassiou, A. Magnetically Driven Floating Foams for the Removal of Oil Contaminants from Water. *ACS Nano* **2012**, *6*, 5413–5419.
- (30) Cao, Y. Z.; Liu, N.; Fu, C. K.; Li, K.; Tao, L.; Feng, L.; Wei, Y. Thermo and pH Dual-Responsive Materials for Controllable Oil/Water Separation. *ACS Appl. Mater. Interfaces* **2014**, *6*, 2026–2030.
- (31) Xiao, M.; Jiang, C.; Shi, F. Design of an UV-Responsive Microactuator on a Smart Device for Light-Induced ON-OFF-ON Motion. *NPG Asia Mater.* **2014**, *6*, 1–8.
- (32) Dong, Y.; Li, J.; Shi, L.; Wang, X. B.; Guo, Z. G.; Liu, W. M. Underwater Superoleophobic Graphene Oxide Coated Meshes for the Separation of Oil and Water. *Chem. Commun.* **2014**, *50*, 5586–5589.
- (33) Xiao, M.; Guo, X. G.; Cheng, M. J.; Ju, G. N.; Zhang, Y. J.; Shi, F. pH-Responsive on-off Motion of a Superhydrophobic Boat: Towards the Design of a Minirobot. *Small* **2014**, *10*, 859–865.
- (34) Xiao, M.; Cheng, M. J.; Zhang, Y. J.; Shi, F. Combining the Marangoni Effect and the pH-Responsive Superhydrophobicity–Superhydrophilicity Transition to Biomimic the Locomotion Process of the Beetles of Genus *Stenus*. *Small* **2013**, *9*, 2509–2514.
- (35) Feng, L.; Zhang, Z. Y.; Mai, Z. H.; Ma, Y. M.; Liu, B. Q.; Jiang, L.; Zhu, D. B. A Super-Hydrophobic and Super-Oleophilic Coating Mesh Film for the Separation of Oil and Water. *Angew. Chem., Int. Ed.* **2004**, *43*, 2012–2014.
- (36) Deng, D.; Prendergast, D. P.; MacFarlane, J.; Bagatin, R.; Stellacci, F.; Gschwend, P. M. Hydrophobic Meshes for Oil Spill Recovery Devices. *ACS Appl. Mater. Interfaces* **2013**, *5*, 774–781.

- (37) Cheng, M. J.; Ju, G. N.; Jiang, C.; Zhang, Y. J.; Shi, F. Magnetically Directed Clean-up of Underwater Oil Spills through a Functionally Integrated Device. *J. Mater. Chem. A* **2013**, *1*, 13411–13416.
- (38) Cheng, M. J.; Gao, Y. F.; Guo, X. P.; Shi, Z. Y.; Chen, J.-F.; Shi, F. A Functionally Integrated Device for Effective and Facile Oil Spill Cleanup. *Langmuir* **2011**, *27*, 7371–7375.
- (39) Wang, F. J.; Lei, S.; Xue, M. S.; Ou, J. F.; Li, C. Q.; Li, W. Superhydrophobic and Superoleophilic Miniature Device for the Collection of Oils from Water Surfaces. *J. Phys. Chem. C* **2014**, *118*, 6344–6351.
- (40) Song, J.; Huang, S.; Lu, Y.; Bu, X.; Mates, J. E.; Ghosh, A.; Ganguly, R.; Carmalt, C. J.; Parkin, I. P.; Xu, W.; Megaridis, C. M. Self-Driven One-Step Oil Removal from Oil Spill on Water via Selective-Wettability Steel Mesh. *ACS Appl. Mater. Interfaces* **2014**, *6*, 19858–19865.
- (41) Wang, C.-F.; Lin, S.-J. Robust Superhydrophobic/Superoleophilic Sponge for Effective Continuous Absorption and Expulsion of Oil Pollutants from Water. *ACS Appl. Mater. Interfaces* **2013**, *5*, 8861–8864.
- (42) Ge, J.; Ye, Y.-D.; Yao, H.-B.; Zhu, X.; Wang, X.; Wu, L.; Wang, J.-L.; Ding, H.; Yong, N.; He, L.-H.; Yu, S.-H. Pumping through Porous Hydrophobic/Oleophilic Materials: An Alternative Technology for Oil Spill Remediation. *Angew. Chem., Int. Ed.* **2014**, *53*, 3612–3616.
- (43) Osherov, A.; Zhu, C. Q.; Panzer, M. J. Role of Solution Chemistry in Determining the Morphology and Photoconductivity of Electrodeposited Cuprous Oxide Films. *Chem. Mater.* **2013**, *25*, 692–698.
- (44) Wang, P.; Ng, Y. H.; Amal, R. Embedment of Anodized p-type Cu₂O Thin Films with CuO Nanowires for Improvement in Photoelectrochemical Stability. *Nanoscale* **2013**, *5*, 2952–2958.
- (45) Kim, S. Y.; Ahn, C. H.; Lee, J. H.; Kwon, Y. H.; Hwang, S.; Lee, J. Y.; Cho, H. K. p-Channel Oxide Thin Film Transistors Using Solution-Processed Copper Oxide. *ACS Appl. Mater. Interfaces* **2013**, *5*, 2417–2421.
- (46) Jiang, T. F.; Xie, T. F.; Yang, W. S.; Chen, L. P.; Fan, H. M.; Wang, D. J. Photoelectrochemical and Photovoltaic Properties of p–n Cu₂O Homojunction Films and Their Photocatalytic Performance. *J. Phys. Chem. C* **2013**, *117*, 4619–4624.
- (47) Yoon, S.; Kim, M.; Kim, I.-S.; Lim, J.-H.; Yoo, B. Manipulation of Cuprous Oxide Surfaces for Improving Their Photocatalytic Activity. *J. Mater. Chem. A* **2014**, *2*, 11621–11627.
- (48) Pan, L.; Zou, J.-J.; Zhang, T. R.; Wang, S. B.; Li, Z.; Wang, L.; Zhang, X. W. Cu₂O Film via Hydrothermal Redox Approach: Morphology and Photocatalytic Performance. *J. Phys. Chem. C* **2014**, *118*, 16335–16343.
- (49) Lee, Y. S.; Heo, J.; Winkler, M. T.; Siah, S. C.; Kim, S. B.; Gordon, R. G.; Buonassisi, T. Nitrogen-Doped Cuprous Oxide as a p-type Hole Transporting Layer in Thin-Film Solar Cells. *J. Mater. Chem. A* **2013**, *1*, 15416–15422.
- (50) Li, C. L.; Li, Y. B.; Delaunay, J.-J. A Novel Method to Synthesize Highly Photoactive Cu₂O Microcrystalline Films for Use in Photoelectrochemical Cells. *ACS Appl. Mater. Interfaces* **2014**, *6*, 480–486.
- (51) Valvo, M.; Rehnlund, D.; Lafont, U.; Hahlin, M.; Edström, K.; Nyholm, L. The Impact of Size Effects on the Electrochemical Behaviour of Cu₂O-Coated Cu Nanopillars for Advanced Li-Ion Microbatteries. *J. Mater. Chem. A* **2014**, *2*, 9574–9586.
- (52) Liu, D. Q.; Yang, Z. B.; Wang, P.; Li, F.; Wang, D. S.; He, D. Y. Preparation of 3D Nanoporous Copper-Supported Cuprous Oxide for High-Performance Lithium Ion Battery Anodes. *Nanoscale* **2013**, *5*, 1917–1921.
- (53) Zhang, Z. H.; Dua, R. B.; Zhang, L. B.; Zhu, H. B.; Zhang, H. N.; Wang, P. Carbon-Layer-Protected Cuprous Oxide Nanowire Arrays for Efficient Water Reduction. *ACS Nano* **2013**, *7*, 1709–1717.
- (54) Bijani, S.; Martínez, L.; Gabás, M.; Dalchiele, E. A.; Ramos-Barrado, J.-R. Low-Temperature Electrodeposition of Cu₂O Thin Films: Modulation of Micro-Nanostructure by Modifying the Applied Potential and Electrolytic Bath pH. *J. Phys. Chem. C* **2009**, *113*, 19482–19487.
- (55) Hassan, I. A.; Parkin, I. P.; Nair, S. P.; Carmalt, C. J. Antimicrobial Activity of Copper and Copper(I) Oxide Thin Films Deposited via Aerosol-Assisted CVD. *J. Mater. Chem. B* **2014**, *2*, 2855–2860.
- (56) Hong, X.; Wang, G. Z.; Zhu, W.; Shen, X. S.; Wang, Y. Synthesis of sub-10 nm Cu₂O Nanowires by Poly(vinyl pyrrolidone)-Assisted Electrodeposition. *J. Phys. Chem. C* **2009**, *113*, 14172–14175.
- (57) Jayawardena, C.; Hewaparakrama, K. P.; Wijewardena, D. L. A.; Guruge, H. Fabrication of n-Cu₂O Electrodes with Higher Energy Conversion Efficiency in a Photoelectrochemical Cell. *Sol. Energy Mater. Sol. Cells* **1998**, *56*, 29–33.
- (58) Fernando, C. A. N.; Wethasinghe, S. K. Investigation of Photoelectrochemical Characteristics of n-Type Cu₂O Films. *Sol. Energy Mater. Sol. Cells* **2000**, *63*, 299–308.
- (59) Shiratsuchi, R.; Hongo, K.; Nogami, G.; Ishimaru, S. Reduction of CO₂ on Fluorine-Doped SnO₂ Thin-Film Electrodes. *J. Electrochem. Soc.* **1992**, *139*, 2544–2549.
- (60) Okamoto, Y.; Carter, W. J.; Hercules, D. M. A Study of the Interaction of Pb-Sn Solder with O₂, H₂O, and NO₂ by X-ray Photoelectron (ESCA) and Auger (AES) Spectroscopy. *Appl. Spectrosc.* **1979**, *33*, 287–293.
- (61) Yao, K. X.; Yin, X. M.; Wang, T. H.; Zeng, H. C. Synthesis, Selfassembly, Disassembly, and Reassembly of Two Types of Cu₂O Nanocrystals Unifaceted with {001} or {110} Planes. *J. Am. Chem. Soc.* **2010**, *132*, 6131–6144.
- (62) Shen, S. L.; Zhuang, J.; Xu, X. X.; Nisar, A.; Hu, S.; Wang, X. Size Effects in the Oriented-Attachment Growth Process: The Case of Cu Nanoseeds. *Inorg. Chem.* **2009**, *48*, 5117–5128.
- (63) Brion, D. Etude Par Spectroscopie de Photoelectrons de la Degradation Superficielle de FeS₂, CuFeS₂, ZnS ET PbS a l'air et Dans l'eau. *Appl. Surf. Sci.* **1980**, *5*, 133–152.
- (64) Dilimon, V. S.; Denayer, J.; Delhalle, J.; Mekhalif, Z. Electrochemical and Spectroscopic Study of the Self-Assembling Mechanism of Normal and Chelating Alkanethiols on Copper. *Langmuir* **2012**, *28*, 6857–6865.
- (65) Bain, C. D.; Biebuyck, H. A.; Whitesides, G. M. Comparison of Self-Assembled Monolayers on Gold: Coadsorption of Thiols and Disulfides. *Langmuir* **1989**, *5*, 723–727.
- (66) Volmer, M.; Statmann, M.; Viehhaus, H. Electrochemical and Electron Spectroscopic Investigations of Iron Surfaces Modified with Thiols. *Surf. Interface Anal.* **1990**, *16*, 278–282.
- (67) Notoya, T. Localized Corrosion in Copper Tubes and the Effect of Anti-Tarnishing Pretreatment. *J. Mater. Sci. Lett.* **1991**, *10*, 389–391.
- (68) Barthlott, W.; Neihuis, C. Purity of the Sacred Lotus, or Escape from Contamination in Biological Surfaces. *Planta* **1997**, *202*, 1–8.
- (69) Nun, E.; Oles, M.; Schleich, B. Lotus-Effect-Surfaces. *Macromol. Symp.* **2002**, *187*, 677–682.
- (70) Guo, Z. G.; Fang, J.; Hao, J.-C.; Liang, Y.-M.; Liu, W.-M. A Novel Approach to Stable Superhydrophobic Surfaces. *ChemPhysChem* **2006**, *7*, 1674–1677.
- (71) Yao, X.; Gao, J.; Song, Y. L.; Jiang, L. Superoleophobic Surfaces with Controllable Oil Adhesion and Their Application in Oil Transportation. *Adv. Funct. Mater.* **2011**, *21*, 4270–4276.
- (72) Zhu, X. T.; Zhang, Z. Z.; Men, X. H.; Yang, J.; Xu, X. H. Rapid Formation of Superhydrophobic Surfaces with Fast Response Wettability Transition. *ACS Appl. Mater. Interfaces* **2010**, *2*, 3636–3641.